Bioorganic Chemistry 91 (2019) 103148

Contents lists available at ScienceDirect

Bioorganic Chemistry

journal homepage: www.elsevier.com/locate/bioorg

Identification of novel peptidomimetics targeting the polo-box domain of polo-like kinase 1

Zhiyan Li[a,b], Zhenguo Zhang[a,b], Huiyong Sun[b], Lili Xu[a,c,*], Cheng Jiang[a,b,c,*]

[a] Jiangsu Key Laboratory of Drug Design and Optimization, China Pharmaceutical University, Nanjing 210009, China
[b] Department of Medicinal Chemistry, China Pharmaceutical University, Nanjing 210009, China
[c] Key Laboratory on Protein Chemistry and Structural Biology, China Pharmaceutical University, Nanjing 210009, China

ARTICLE INFO

Keywords:
Polo-like kinase 1
Polo-box domain
Plk1 PBD
Inhibitors
Unnatural amino acid

ABSTRACT

A series of new peptidomimetics targeting the polo-box domain (PBD) of polo-like kinase 1 (Plk1) was identified based on the potent and selective pentapeptide Plk1 PBD inhibitor PLHSpT. Unnatural amino acid residues were introduced to the newly designed compound and the *N*-terminal substituent of the peptidomimetic was investigated. The optimized compound **9** inhibited the Plk1 PBD with IC_{50} of 0.267 μM and showed almost no inhibition to Plk2 PBD or Plk3 PBD at 100 μM. Biolayer interferometry studies demonstrated that compound **9** showed potent binding affinity to Plk1 with a K_d value of 0.164 μM, while no K_d were detected against Plk2 and Plk3. Compound **9** showed improved stability in rat plasma compared to PLHSpT. Binding mode analysis was performed and in agreement with the observed experimental results. There are only two natural amino acids remained in the chemical structure of **9**. This study may provide new information for further research on Plk1 PBD inhibitors.

1. Introduction

Polo-like kinases (Plks) are highly conserved families of serine/threonine protein kinases that are essential for multiple processes in the cell cycle progression, among which Plk1 is most thoroughly characterized [1,2]. Plk1 regulates several key mitotic events, such as mitotic entry, centrosome maturation, spindle assembly, chromosome segregation, and cytokinesis [1–3]. Plk1 is overexpressed in a broad spectrum of cancer types, which often correlates with poor prognosis [4]. Overexpression of Plk1 in cancer cells, but not in normal cells, makes it an attractive and hot therapeutic target.

Among the five identified mammalian Plk family members (Plk1-5), Plk1-4 consists of an *N*-terminal catalytic domain and a highly conserved *C*-terminal domain composed of 1 or 2 highly conserved sequences, termed polo-box domains (PBDs) [5,6]. PBD directs the *N*-terminal catalytic domain for specific subcellular localization through interacting with phosphoserine/phosphothreonine (pS/pT)-containing motifs [7].

Plk1, Plk2 and Plk3 are closely related while Plk4 is a less related kinase which apparently expressed in different patterns and showed different physiological functions [4,8]. However, Plk2 and Plk3, two most closely related kinases with Plk1, appear to function as oncogenic suppressors [4,7,8]. Several potent ATP-competitive Plk1 inhibitors targeting the ATP-binding catalytic domain have been reported. However, ATP-binding pockets of Plks have high similarities, therefore it is difficult to target Plk1 specifically [9]. An alternative approach for identifying potent and highly selective Plk1 inhibitors is to target the PBD which is unique and a specific signature of the Plks [10]. Therefore the inhibition of Plk1 PBD is considered to be an effective method of inhibiting Plk1, which can avoid related specificity problems [11,12].

A phosphothreonine (pT)-containing pentapeptide PLHSpT (Fig. 1, 1) was identified as a potent Plk1 PBD inhibitor (Plk1 PBD K_d = 0.445 μM, no binding to Plk2 PBD) [5]. After that, several phosphate peptides and peptidomimetics were reported (Fig. 1, 2–4) [13–21]. A series of (2*S*,3*R*)-2-amino-3-methyl-4-phosphonobutanoic acid (Pmab) incorporated peptidomimetic analogues was also reported as a phosphatase-stable peptidomimetic with potent inhibition to Plk1 PBD [22]. Representative compound (Fig. 1, 5) showed potent Plk1 inhibitory activity (Plk1 PBD IC_{50} = 0.21 μM) and high selectivity (Plk2 PBD IC_{50} > 1000 μM, Plk3 PBD IC_{50} > 1000 μM). However, these reported peptides and peptidomimetics with potent and highly selective Plk1 PBD inhibition have several issues such as limited bioavailability, and poor plasma stability, et al. [19]. In our previous study, a series of D-amino acid-containing peptidomimetics were identified as novel polo-like kinase 1 (Plk1) polo-box domain (PBD) inhibitors. Among which compound **6** (Fig. 1) showed potent Plk1 inhibitory activity (Plk1 PBD

* Corresponding authors at: Jiangsu Key Laboratory of Drug Design and Optimization, China Pharmaceutical University, Nanjing 210009, China.
E-mail addresses: 1620174420@cpu.edu.cn (L. Xu), jc@cpu.edu.cn (C. Jiang).

https://doi.org/10.1016/j.bioorg.2019.103148
Received 28 April 2019; Received in revised form 9 July 2019; Accepted 23 July 2019
Available online 27 July 2019

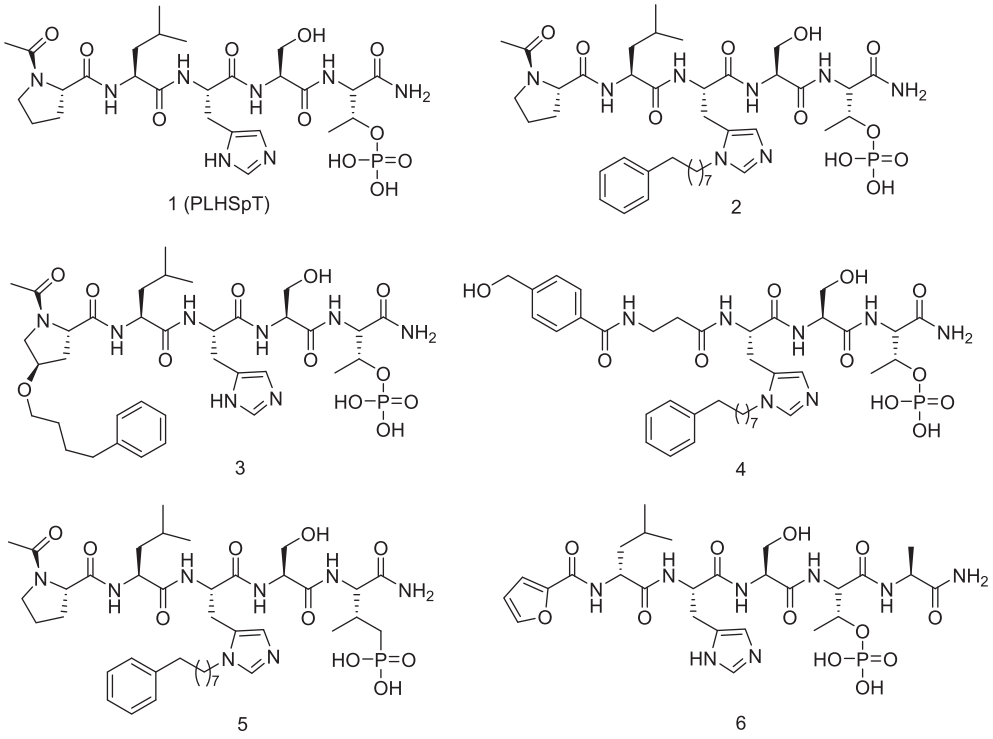

Fig. 1. Representative reported phosphate peptides and peptidomimetics as Plk1 PBD inhibitors.

IC_{50} = 0.80 μM) and high selectivity (Plk2 PBD IC_{50} > 100 μM, Plk3 PBD IC_{50} > 100 μM), together with improved stability in rat plasma compared to L-peptide inhibitor [23].

In this study, the Pro and Leu in the *N*-terminal and the His residue of PLHSpT were modified respectively. A series of potent and selective Plk1 PBD inhibitors with only two natural amino acid residues remained were identified.

2. Results and discussion

2.1. Design, synthesis and evaluation

The reported potent and selective pentapeptide (PLHSpT) was selected as a lead, and a series of modifications were explored in order to discover more minimal peptide. Firstly, carboxylic acid group was introduced to the *N*-terminal Pro-Leu residues considering there is a basic amino acid residue Arg516 in the pyrrolidine-binding region of Plk1 PBD [17]. Thus compound **7a** to **7d** was designed and synthesized. The four obtained compounds were evaluated using our optimized fluorescence polarization (FP) method. As shown in Table 1, the binding affinity of the four compounds to Plk1 PBD decreased dramatically. Then the *N*-terminal Leu was kept and modifications on the Pro was explored using the same method as the design of **7a** to **7d**. Compound **7e** to **7h** was obtained as list in Table 1. It could be found that compound **7e**, in which that an L-Asp was introduced and taken the place of Pro in PLHSpT, showed comparable Plk1 PBD binding affinity as PLHSpT. However, the amino acid residues which take the place of the *N*-terminal Pro-Leu residues in PLHSpT were still natural amino acids, they have several issues such as limited bioavailability, and poor plasma stability, et al. [19]. In order to overcome these weakness, the amino acids of the parental peptide could be substituted with unnatural amino acids. Ann et al. has reported the discovery of a series of peptidomimetics targeting Plk1 PBD, the *N*-terminal Pro-Leu residues was replaced by substituted beta amino acid [19]. 4-Hydroxymethyl-benzoic acid was considered as an optimized *N*-terminal substitution in this modification [19]. Based on this result, compound **7i** was designed, synthesized and evaluated, which showed moderate binding affinity to Plk1 PBD (IC_{50} = 2.632 μM). Then carboxyl group was introduced to the *N*-terminal 4-hydroxymethyl benzoyl substituted beta amino acid and compound **7j** and **7k** were obtained. As shown in Table 1, compound **7k**, with a (*S*)-configuration *N*-terminal 'tail' showed potent Plk1 PBD inhibition (IC_{50} = 0.648 μM). Isoform selectivity evaluation showed that compound **7k** showed almost no binding to Plk2 PBD and Plk3 PBD at 100 μM.

Then, the His residue in PLHSpT was modified by changing the imidazole ring to other aromatic or heterocyclic groups and compound **8a** to **8f** were designed and synthesized. Compound **8a** with a phenyl replaced imidazole showed moderate Plk1 PBD inhibitory activity (IC_{50} = 4.779 μM), while compound **8d**, **8e** and **8f** containing a pyridine-4-yl, thiophen-2-yl and thiazol-4-yl replaced imidazole showed potent Plk1 PBD inhibitory activity with IC_{50} of 0.586, 0.511 and 0.441 μM respectively.

Finally, the optimized *N*-terminal 'tail' was introduced to take the place of Pro-Leu in **8f** and compound **9** was obtained. Compound **9** showed potent Plk1 PBD inhibition with an IC_{50} of 0.267 μM (Table 1 and Supporting Information). The binding affinity of **9** for Plk2 PBD and Plk3 PBD was evaluated in our FP assay (Supporting Information). As shown in Table 1, compound **9** showed almost no binding to Plk2 PBD and Plk3 PBD at 100 μM. The newly identified peptidomimetic **9** showed excellent selectivity to Plk1 PBD against Plk2 PBD and Plk3 PBD.

To better describe the inhibitory activity for compound **9**, we performed the biolayer interferometry (BLI) studies and compared binding affinities of compound **9** to Plk1, Plk2 and Plk3. This study demonstrated that compound **9** showed a K_d value of 0.164 μM against Plk1 (Fig. 2), while no K_d were detected against Plk2 and Plk3.

2.2. Plasma stability

The stability of PLHSpT (**6**) and optimized compound **9** were determined following time-dependent incubation in rat plasma using LC-MS. As shown in Fig. 3, the degradation of compound **9** is significantly (p < 0.05) slower than PLHSpT after 60 min and longer incubation. By 120 min, 73.9% of PLHSpT retained in plasma, while more than 85%

Table 1
Structures of designed compounds and inhibitory activity to Plk1 PBD, Plk2 PBD and Plk3 PBD.

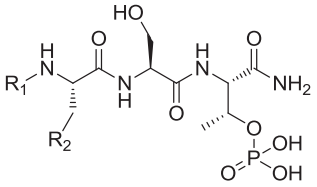

Compound	R_1	R_2	Plk1 PBD IC_{50} (μM)[a]	Plk2 PBD IC_{50} (μM)[a]	Plk3 PBD IC_{50} (μM)[a]
PLHSpT (**1**)	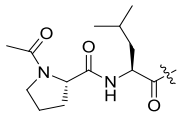		0.526 ± 0.013	> 100	> 100
7a	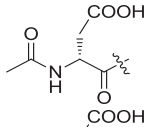		24.78 ± 1.24	N.D.	N.D.
7b	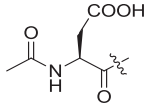		133.6 ± 4.1	N.D.	N.D.
7c	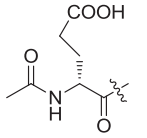		4.396 ± 0.184	N.D.	N.D.
7d	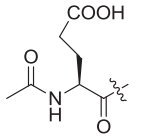		110.2 ± 3.3	N.D.	N.D.
7e	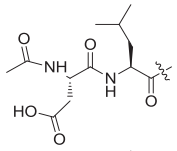		0.791 ± 0.233	> 100	> 100
7f	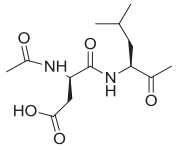		4.200 ± 0.847	N.D.	N.D.
7g	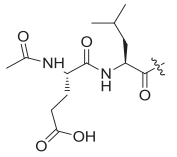		17.73 ± 1.56	N.D.	N.D.
7h	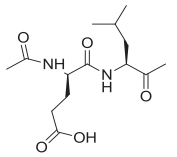		2.813 ± 0.618	N.D.	N.D.
7i	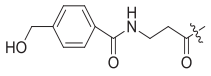		2.632 ± 0.719	N.D.	N.D.
7j	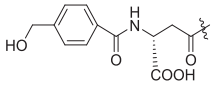		6.374 ± 1.021	N.D.	N.D.
7k	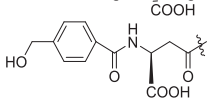		0.648 ± 0.039	> 100	> 100

(*continued on next page*)

Table 1 (*continued*)

Compound	R_1	R_2	Plk1 PBD IC_{50} (μM)[a]	Plk2 PBD IC_{50} (μM)[a]	Plk3 PBD IC_{50} (μM)[a]
8a	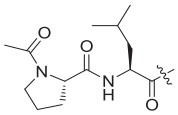		4.779 ± 0.882	N.D.	N.D.
8b	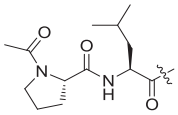		1.947 ± 0.665	N.D.	N.D.
8c	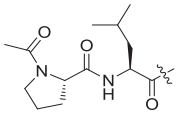		1.172 ± 0.504	N.D.	N.D.
8d	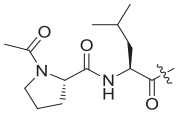	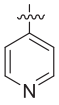	0.586 ± 0.075	> 100	> 100
8e	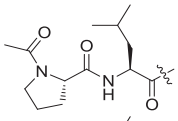		0.511 ± 0.058	> 100	> 100
8f	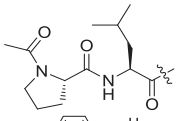		0.441 ± 0.009	> 100	> 100
9	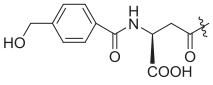		0.267 ± 0.036	> 100	> 100

N.D.: Not Determined.

[a] IC_{50} Values represent the mean of at least three independent determinations.

for compound **9** remained in comparison. This result demonstrated that compound **9** have improved stability in rat plasma compared to PLHSpT (**1**).

2.3. Binding mode analysis

Routine methods based on molecular docking were used for analyzing the binding mode of compound **9** [24–26]. As shown in Fig. 4, consistent binding modes were found between compound **9** (yellow) and the co-crystallized ligand PLSHpT (**1**, cyan) in structure of PDB 3HIK. The negatively charged phosphate group of phosphorylated threonine residue in the two compounds both form electrostatic interactions with Lys540 (2.9 Å, right panel in Fig. 4). The carbonyl oxygen of the *N*-terminal proline residue of PLSHpT was in polar contact (H bond) with the guanidinium moiety of Arg516, while the newly introduced negatively charged carboxyl group in compound **9** can form an electrostatic interaction with the guanidinium moiety Arg516 (2.9 Å, left panel in Fig. 4), which enhances the binding affinity of compound **9** to Plk1 PBD.

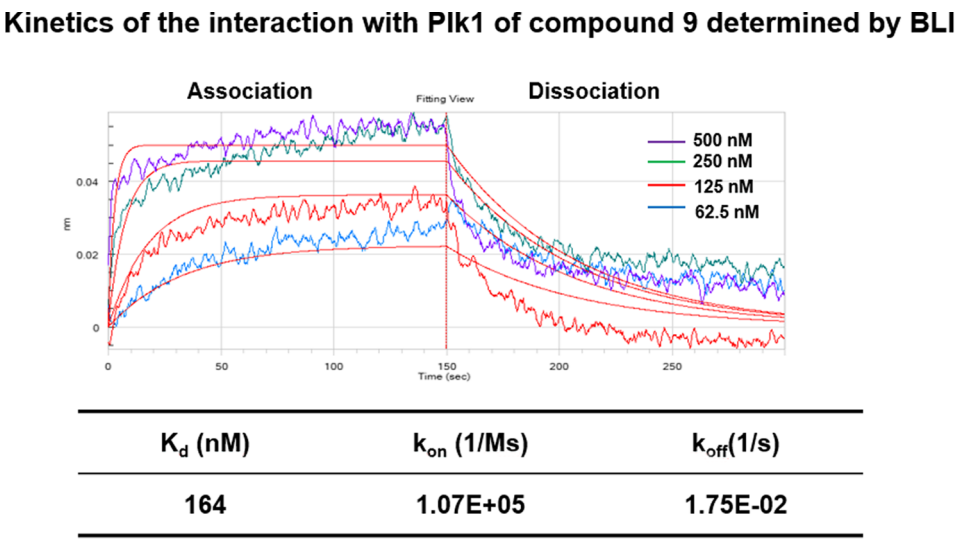

Fig. 2. Biolayer interferometry sensorgrams of the binding of varying concentrations of the Plk1 protein to compound **9**.

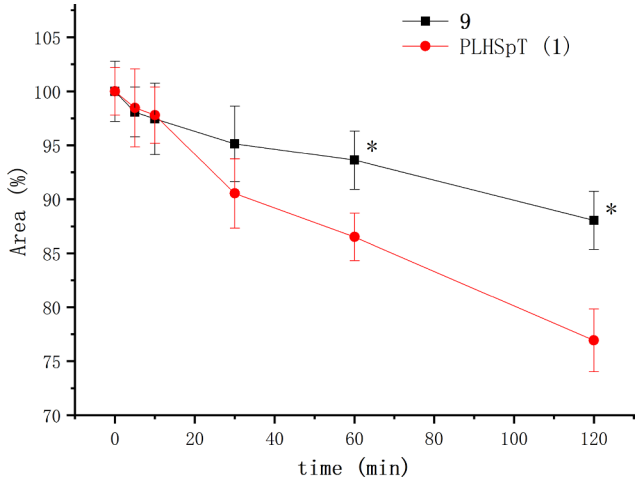

Fig. 3. Plasma stability of compound **1** and **9**[a]. [a]Statically significant different ($p < 0.05$) for area% of compound **1** and **9**. Data was tested by One-way ANOVA.

3. Conclusion

We have designed and synthesized a series of peptidomimetics as new Plk1 PBD inhibitors. Binding affinity of the synthesized compounds was evaluated using our optimized FP assay. Among the 18 compounds obtained, 6 compounds (**7e**, **7k**, **8d**, **8e**, **8f** and **9**) showed potent Plk1 PBD inhibitory activity with IC_{50} less than 1 μM. Specially, compound **9** was the most potent one which inhibited Plk1 PBD with an IC_{50} at 0.267 μM, and almost no inhibition to Plk2 PBD or Plk3 PBD at 100 μM. Biolayer interferometry studies demonstrated that compound **9** showed potent binding affinity to Plk1 with a K_d value of 0.164 μM, while no binding detected against Plk2 and Plk3. Additionally, compound **9** had improved stability in rat plasma compared to PLHSpT (**1**) which confirmed our hypothesis of plasma-stable unnatural amino acid modification. Binding mode analysis was performed and it was found that the negatively charged carboxyl group introduced to the *N*-terminal can form an electrostatic interaction with the guanidinium moiety Arg516, which can enhance the binding affinity to Plk1 PBD. In this work, from the lead with five natural amino acids, potent and selective Plk1 PBD inhibitor with only two natural amino acids left in the structure was identified. This work can provide a new idea and method for the further research of Plk1 PBD inhibitors as potential anticancer therapy.

4. Experimental section

4.1. Chemistry

Rink amide 4-methylbenzhydrylamine resin and 9-fluorenylmethoxycarbonyl (Fmoc) amino acids were obtained from Jill Biochemical Co., Ltd. Other reagents used for peptide synthesis included trifluoroacetic acid (TFA; Aladdin Reagent Co., Ltd), piperidine (Sinopharm Chemical Reagent Co., Ltd), 1-*O*-benzotriazole- *N*,*N*,*N*′,*N*′-tetramethyluronium hexafluoro-phosphate (HBTU; Jill Biochemical Co., Ltd), 1- hydroxybenzotriazole hydrate (HOBt; Jill Biochemical Co., Ltd), and *N*,*N*- dimethylformamide (DMF, peptide synthesis grade; Tianjin Chemical Reagent Factory).

All peptides were prepared by Fmoc SPPS methods using Rink amide with an initial loading of 0.8 mmol/g unless otherwise noted. Fmoc-Ser(*t*-Bu)-OH and other Fmoc protected amino acids were purchased from Jill Biochemical Co., Ltd. Resins were swollen in *N*,*N*-dimethylformamide (DMF) for 30 min prior to synthesis. For sequence extension, the Fmoc-protected amino acid (3.0 equiv) was activated by treatment with HBTU (3.0 equiv), HOBt (3.0 equiv) and *N*,*N*-diisopropylethylamine (6.0 equiv) in DMF (1 mL) for 2 min. This solution was added to the free amine on resin, and the coupling reaction was allowed to proceed for 1 h with vortex stirring. After washing with DMF, Fmoc deprotection was achieved with 20% piperidine in DMF (1 × 10 min, 1 × 15 min). The resin was washed once again, and the process was repeated for the next amino acid, and finally the resin was washed with DMF, dichloromethane and then dried under vacuum. Linear peptides were cleaved from the resin with 5% triisopropylsilane (TIS) and 5% H_2O in trifluoroacetic acid (TFA, approximately 2 mL of TFA per 100 mg of resin) for 3 h. The cleavage mixture was mixed with cold ether to precipitate the peptide and then centrifugation. Reverse-phase HPLC analysis (RP-HPLC) was carried out on the preparative Vydac C18 column (15 μm, 20 mm × 250 mm) using an appropriate water/acetonitrile gradient in the presence of 0.1% TFA. The final purity of the peptides (> 95%) was assessed by RP-HPLC on an analytical Vydac C18 column (4.6 mm × 250 mm, 300 Å, 5 μm particle size). The molecular masses of purified peptides were determined using ESI-MS (Thermo-Finnigan, San Jose, CA, USA).

Compound 7a. HRMS (ESI-TOF) *m/z* calc'd for $C_{19}H_{30}N_7O_{12}P$ [M + H]$^+$ 580.1846, found 580.1851, Purity > 99%;
Compound 7b. HRMS (ESI-TOF) *m/z* calc'd for $C_{19}H_{30}N_7O_{12}P$ [M + H]$^+$ 580.1846, found 580.1848, Purity > 99%;
Compound 7c. HRMS (ESI-TOF) *m/z* calc'd for $C_{20}H_{32}N_7O_{12}P$ [M + H]$^+$ 594.1936, found 594.1931, Purity > 99%;

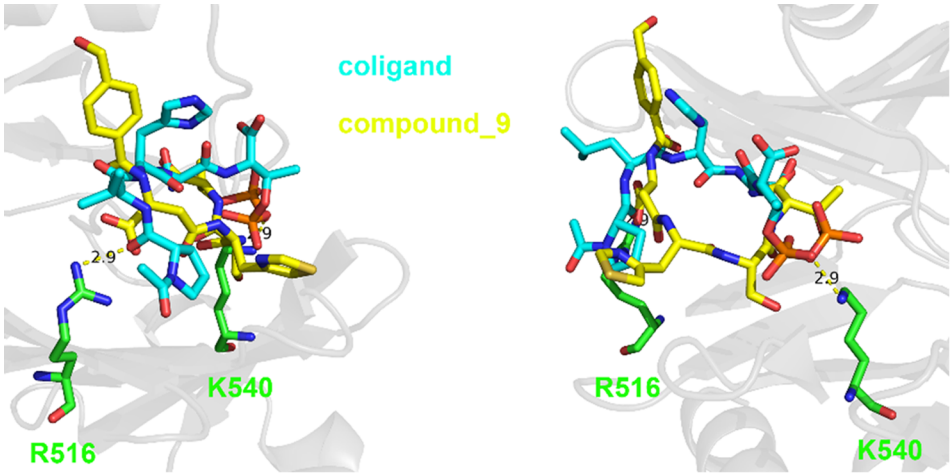

Fig. 4. Binding modes of compound **9** (yellow) and the co-crystallized ligand PLHSpT (cyan), where consistent binding modes were found between compound **9** and PLHSpT in the crystal structure (PDB code 3HIK).

Compound 7d. HRMS (ESI-TOF) *m/z* calc'd for $C_{20}H_{32}N_7O_{12}P$ [M + H]$^+$ 594.1936, found 594.1941, Purity > 99%;
Compound 7e. HRMS (ESI-TOF) *m/z* calc'd for $C_{25}H_{41}N_8O_{13}P$ [M + H]$^+$ 693.2609, found 693.2609, Purity > 98%;
Compound 7f. HRMS (ESI-TOF) *m/z* calc'd for $C_{25}H_{41}N_8O_{13}P$ [M + H]$^+$ 693.2609, found 693.2604, Purity > 98%;
Compound 7 g. HRMS (ESI-TOF) *m/z* calc'd for $C_{26}H_{43}N_8O_{13}P$ [M + H]$^+$ 707.2760, found 707.2757, Purity > 96%;
Compound 7 h. HRMS (ESI-TOF) *m/z* calc'd for $C_{24}H_{41}N_8O_{11}P$ [M + H]$^+$ 707.2760, found 707.2764, Purity > 96%;
Compound 7i. HRMS (ESI-TOF) *m/z* calc'd for $C_{24}H_{34}N_7O_{11}P$ [M + H]$^+$ 628.2172, found 628.2176, Purity > 99%;
Compound 7j. HRMS (ESI-TOF) *m/z* calc'd for $C_{25}H_{34}N_7O_{13}P$ [M + H]$^+$ 672.2054, found 672.2049, Purity > 98%;
Compound 7 k. HRMS (ESI-TOF) *m/z* calc'd for $C_{25}H_{34}N_7O_{13}P$ [M + H]$^+$ 672.2054, found 672.2055, Purity > 98%;
Compound 8a. HRMS (ESI-TOF) *m/z* calc'd for $C_{29}H_{45}N_6O_{11}P$ [M + H]$^+$ 685.2942, found 685.2945, Purity > 98%;
Compound 8b. HRMS (ESI-TOF) *m/z* calc'd for $C_{28}H_{44}N_7O_{11}P$ [M + H]$^+$ 686.2924, found 686.2928, Purity > 98%;
Compound 8c. HRMS (ESI-TOF) *m/z* calc'd for $C_{28}H_{44}N_7O_{11}P$ [M + H]$^+$ 686.2924, found 686.2919, Purity > 98%;
Compound 8d. HRMS (ESI-TOF) *m/z* calc'd for $C_{28}H_{44}N_7O_{11}P$ [M + H]$^+$ 686.2924, found 686.2924, Purity > 99%;
Compound 8e. HRMS (ESI-TOF) *m/z* calc'd for $C_{27}H_{43}N_6O_{11}SP$ [M + H]$^+$ 691.2526, found 691.2527, Purity > 98%;
Compound 8f. HRMS (ESI-TOF) *m/z* calc'd for $C_{26}H_{42}N_7O_{11}SP$ [M + H]$^+$ 692.2449, found 692.2453, Purity > 99%;
Compound 9. HRMS (ESI-TOF) *m/z* calc'd for $C_{25}H_{33}N_6O_{13}SP$ [M + H]$^+$ 689.1642, found 689.1641, Purity > 98%;

4.2. Fluorescence polarization (FP) assays

The binding experiments were performed on a SpectraMax MultiMode Microplate Reader (Molecular Devices) using the excitation at 485 nm and emission filters at 535 nm, respectively. In the fluorescein polarization assays, FP was determined by measuring intensities parallel (Intparallel, F‖) and the perpendicular fluorescence intensity (Intperpendicular, F⊥). The percentage inhibition of the phosphopeptides at each concentration was defined as $= 1 - (P_{obs} - P_{min})/(P_{max} - P_{min})$. Where, P_{max} was the polarization of the wells containing Plk1 PBD and the probe, P_{min} was referred to the polarization of the free probe, and the P_{obs} was the polarization for the wells containing the inhibitors at a range of concentrations under the assay conditions. Briefly, FITC-GPMQSpTPLNG-OH was used as the Fluorescein-labeled peptides (fluorescent probe, purity > 95%) as previously reported, which was dissolved in dimethyl sulfoxide (DMSO) and the finally optimized concentration was set at 20 nM. Phosphopeptides used for competition binding assays were dissolved in assay buffer. The buffer makes up 10 mM NaCl, 50 mM Tris (pH 8.0), 1 mM EDTA-2Na. We further performed the sensitivity by synthesizing two new fluorescent probes, FITC-GPMQTSpTPKNG-OH for Plk2 PBD and FITC-GPLATSpTPKNG-OH for Plk3 PBD, respectively.

Binding-affinities experiments were performed in 384-well, black, round microtiter bottom plates (Corning 3575, Thermo Scientific), which were filled with 20 μL of 60 nM FITC-GPMQSpTPLNG-OH, 20 μL of 4 μM Plk1 PBD, 20 μL of tested phosphopeptides at varying concentrations in assay buffer. A well containing no Plk1 PBD was served as a blank control whereas the negative control including Plk1 PBD, probe complex and assay buffer (equivalent to 0% inhibition). The 384-well black plate was incubated at room temperature for 30 min with gentle shaking prior to FP values measurements. However, the Plk2 PBD or Plk3 PBD was introduced into the selectivity assays to replace Plk1 PBD. All experiments were performed in triplicate. Competition binding data were analyzed using GraphPad Prism 6.0 software (GraphPad Software, San Diego, CA) and the inhibition constants (IC_{50}) were calculated by nonlinear curve fitting.

4.3. Biolayer interferometry assay

Biolayer interferometry (BLI) assay was conducted based on methods previously described [27]. The interactions of the compound **9** with Plk1, Plk2 and Plk3 protein were detected by biolayer interferometry using an Octet Red 96 instrument (FortéBio, MenloPark, CA, USA). Plk1, Plk2 and Plk3 protein were biotinylated with one molar ratio using EZ link sulfo-NHS-LC-biotinylation kit (#21340, Thermo Pierce). Super Streptavidin biosensors tips (FortéBio, Inc., Menlo Park, CA) were prewetted with BLI kinetics buffer (PBS, 0.05% BSA, 0.01% Tween-20) for 10 mins to establish a baseline before immobilization. Then biotinylated protein was bound by dipping SSA sensors into biotinylated Plk1, Plk2 or Plk3 protein (a final concentration of 200 nM). Then four concentrations of compound **9** prepared in BLI kinetics buffer was immobilized onto SSA sensors. All of the binding data were collected at 30 °C. The experiments comprised five steps: (1) baseline acquisition (60 s), (2) protein loading onto the sensor (1000 s), (3) second baseline acquisition (120 s), (4) association of compound for the measurement of k_{on} (150 s), and (5) dissociation of compound for the measurement of k_{off} (150 s). Baseline and dissociation steps were performed in buffer only. The association and dissociation plot and kinetic constants (k_{on} and k_{off}) were step corrected, reference corrected, fit globally to a 1:1 binding model and automatically obtained with Octet data analysis software (7.1). Equilibrium dissociation constants (K_d) were calculated by the ratio of k_{off} to k_{on}.

4.4. Plasma stability

One milliliter of rat plasma was mixed with 0.1 mL compound **6** or compound **18** solution to make a final concentration of 10 μg·mL^{-1}. The mixture was incubated at 37 °C. An aliquot of 100 μL solution was taken at different time interval and mixed with 300 μL of methanol acetonitrile (50:50, v/v) to precipitate plasma proteins. After vortexed and centrifuged at 4 °C for 20 min at 12,000 rpm. The supernatant was transferred and determined with LC-MS.

The LC-MS analysis was performed by a Thermo TSQ Quantis LC-MS/MS system (Thermo, US), consisting of a binary pump solvent management system, an online degasser, an autosampler, and a TSQ Quantum mass spectrometry. The chromatographic separation was performed with an InertSustain C18 column (150 × 4.6 mm, 5 μm) with a gradient mobile phase of 0.1% formic acid in water (solvent A) and 0.1% formic acid in acetonitrile (solvent B). The gradient program was as follows: 0 min 5% B; 8 min 30% B; 8.2 min 80% B; 9 min 80% B; 9.1 min 5% B; 15 min 5% B, and the flow rate was 1 mL min^{-1}. All the samples were studied with an injection volume of 20 μL.

Positive electrospray ionization (ESI) mode was used for the MS determination, with the source parameters were as follows: spray voltage, 4000 V; transfer tube temperature, 350 °C; sheath gas 30 Arb; ion sweep gas pressure 1.0 psi.

4.5. Molecular modeling

In this study, Autodock 4.2 with Lamarckian genetic algorithm (LGA) was employed for molecular docking due to its good performance in reproducing the binding mode of a ligand to its target [24]. The PDB structure of 3HIK was used as the receptor for molecular docking. The Gasteiger partial charge was assigned to the system of interest. The docking space was set to 18.75 × 18.75 × 18.75 Å^3 (corresponding to 50 × 50 × 50 grids, with each grid 0.375 Å in length) for sufficient sampling. Each ligand was docked for 50 times to derive the most stable docking pose for analysis.

Acknowledgements

This work has been financially supported by National Natural Science Foundation of China (No. 81573278) and Excellent Science and Technology Innovation Team Projects of Jiangsu Province Universities in 2017.

Appendix A. Supplementary material

Supplementary data to this article can be found online at https://doi.org/10.1016/j.bioorg.2019.103148.

References

[1] V. Archambault, D.M. Glover, Polo-like kinases: conservation and divergence in their functions and regulation, Nat. Rev. Mol. Cell Biol. 10 (2009) 265–675.
[2] K. Strebhardt, Multifaceted polo-like kinases: drug targets and antitargets for cancer therapy, Nat. Rev. Drug Discov. 9 (2010) 643–660.
[3] M. Petronczki, P. Lenart, J.M. Peters, Polo on the rise-from mitotic entry to cytokinesis with Plk1, Dev. Cell 14 (2008) 646–659.
[4] K. Strebhardt, A. Ullrich, Targeting polo-like kinase 1 for cancer therapy, Nat. Rev. Cancer 6 (2006) 321–330.
[5] S.M. Yun, T. Moulaei, D. Lim, J.K. Bang, J.E. Park, S.R. Shenoy, F. Liu, Y.H. Kang, C.Z. Liao, N.K. Soung, S. Lee, D.Y. Yoon, Y. Lim, D.H. Lee, A. Otaka, E. Appella, J.B. McMahon, M.C. Nicklaus, T.R. Burke, M.B. Yaffe, A. Wlodawer, K.S. Lee, Structural and functional analyses of minimal phosphopeptides targeting the polo-box domain of polo-like kinase 1, Nat. Struct. Mol. Biol. 16 (2009) 876–882.
[6] D.G. Carcer, G. Manning, M. Malumbres, From Plk1 to Plk5: functional evolution of polo-like kinases, Cell Cycle 10 (2011) 2255–2262.
[7] Y.J. Jang, C.Y. Lin, S. Ma, R.L. Erikson, Functional studies on the role of the C-terminal domain of mammalian polo-like kinase, Pro. Natl. Acad. Sci. U. S. A. 99 (2002) 1984–1989.
[8] D.M. Lowery, D. Lim, M.B. Yaffe, Structure and function of Polo-like kinases, Oncogene 24 (2005) 248–259.
[9] M.E. Noble, J.A. Endicott, L.N. Johnson, Protein kinase inhibitors: insights into drug design from structure, Science 303 (2004) 1800–1805.
[10] W.L. DeLano, M.H. Ultsch, A.M. deVos, J.A. Wells, Convergent solutions to binding at a protein-protein interface, Science 287 (2000) 1279–1283.
[11] C. McInnes, M.D. Wyatt, PLK1 as an oncology target: current status and future potential, Drug Discov. Today 16 (2011) 619–625.
[12] S.M. Lens, E.E. Voest, R.H. Medema, Shared and separate functions of polo-like kinases and aurora kinases in cancer, Nat. Rev. Cancer 10 (2010) 825–841.
[13] F. Liu, J.E. Park, W.J. Qian, D. Lim, M. Garber, M.B. Yaffe, K.S. Lee, T.R. Burke Jr., Serendipitous alkylation of a Plk1 ligand uncovers a new binding channel, Nat. Chem. Biol. 7 (2011) 595–601.
[14] R.N. Murugan, J.E. Park, E.H. Kim, S.Y. Shin, C. Cheong, K.S. Lee, J.K. Bang, Plk1-targeted small molecule inhibitors: molecular basis for their potency and specificity, Mol. Cells 232 (2011) 209–220.
[15] F. Liu, J.E. Park, W.J. Qian, D. Lim, A. Scharow, T. Berg, M.B. Yaffe, K.S. Lee, T.R. Burke Jr., Identification of high affinity polo-like 1 (Plk1) polo-box domain binding peptides using oxime-based diversification, ACS Chem. Biol. 7 (2012) 805–810.
[16] F. Liu, J.E. Park, W.J. Qian, D. Lim, A. Scharow, T. Berg, M.B. Yaffe, K.S. Lee, T.R. Burke Jr., Peptoid-peptide hybrid ligands targeting the polo box domain of polo-like kinase 1, ChemBioChem 13 (2012) 1291–1296.
[17] R.N. Murugan, J.E. Park, D. Lim, M. Ahn, C. Cheong, T. Kwon, K.Y. Nam, S.H. Choi, B.Y. Kim, D.Y. Yoon, M.B. Yaffe, D.Y. Yu, K.S. Lee, J.K. Bang, Development of cyclic peptomer inhibitors targeting the polo-box domain of polo-like kinase 1, Bioorg. Med. Chem. 21 (2013) 2623–2634.
[18] X.Z. Zhao, D. Hymel, T.R. Burke Jr., Application of oxime-diversification to optimize ligand interactions within a cryptic pocket of the polo-like kinase 1 polo-box domain, Bioorg. Med. Chem. Lett. 26 (2016) 5009–5012.
[19] M. Ahn, Y.H. Han, J.E. Park, S. Kim, W.C. Lee, S.J. Lee, P. Gunasekaran, C. Cheong, S.Y. Shin Sr., H.Y. Kim, E.K. Ryu, R.N. Murugan, N.H. Kim, J.H. Bang, A new class of peptidomimetics targeting the polo-box domain of polo-like kinase 1, J. Med. Chem. 58 (2015) 294–304.
[20] W.J. Qian, J.E. Park, K.S. Lee, T.R. Burke Jr., Non-proteinogenic amino acids in the pThr-2 position of a pentamer peptide that confer high binding affinity for the polo box domain (PBD) of polo-like kinase 1 (Plk1), Bioorg. Med. Chem. Lett. 22 (2012) 7306–7308.
[21] X.Z. Zhao, D. Hymel, T.R. Bruke Jr., Enhancing polo-like kinase 1 selectivity of polo-box domain-binding peptides, Bioorg. Med. Chem. 25 (2017) 5041–5049.
[22] D. Hymel, T.R. Burke Jr., Phosphatase-stable phosphoamino acid mimetics that enhance binding affinities with the polo-box domain of polo-like kinase 1, ChemMedChem 12 (2017) 202–206.
[23] Z.Y. Li, Z.G. Zhang, Y.H. Chen, S.J. Tang, T.Y. Lin, J.F. Huang, B. Li, C. Jiang, Design, synthesis and evaluation of *d*-amino acid-containing peptidomimetics targeting the polo-box domain of polo-like kinase 1, Bioorg. Chem. 85 (2019) 534–540.
[24] G.M. Morris, R. Huey, W. Lindstrom, M.F. Sanner, R.K. Belew, D.S. Goodsell, A.J. Olson, AutoDock4 and AutoDockTools4: automated docking with selective receptor flexibility, J. Comput. Chem. 30 (2009) 2785–2791.
[25] H. Sun, P. Chen, D. Li, Y. Li, T. Hou, Directly-binding rather than Induced-fit dominated binding affinity difference in (*S*) and (*R*)-crizotinib bound MTH1, J. Chem. Theory Comput. 12 (2016) 851–860.
[26] H. Sun, P. Pan, S. Tian, L. Xu, X. Kong, Y. Li, D. Li, T. Hou, Constructing and validating high-performance MIEC-SVM models in virtual screening for kinases: a better way for actives discovery, Sci. Rep. 6 (2016) 24817.
[27] F. Jiang, A.P. Guo, J.C. Xu, Q.D. You, X.L. Xu, Discovery of a potent Grp94 selective inhibitor with anti-inflammatory efficacy in a mouse model of ulcerative colitis, J. Med. Chem. 61 (2018) 9513–9533.